CONSTRUCTION OF PLANT BIOLOGICAL CIRCUIT MODEL FOR STORING MODAL INFORMATION DURING TOMATO GROWTH PROCESS
/
番茄生长过程储存模态信息的植株生物电路模型构建

Ying WANG[1)], Huifei YANG[2)], Ruijie XIE[2)], Zhenyu LIU*[2)]
[1)] College of Agricultural Engineering, Shanxi Agricultural University, Taigu / China;
[2)] College of Information Science and Engineering, Shanxi Agricultural University, Taigu / China
Tel: +86-0354-6288165; E-mail: lzysyb@126.com

DOI: https://doi.org/10.35633/inmateh-68-81

Keywords: *tomato plant, parameter inversion, dielectric characteristics, modal information, circuit model*

ABSTRACT
During the growth and development of tomato plants, its different cells or tissues would store external environmental information and express it in the form of ion transportation. In order to better examine the storage model of tomato plants, the tomato individual tissue and whole plant biological circuit models were closely examined based on the idea of modal theory. According to the parameter inversion theory, in the frequency range of 0.1Hz - 1MHz, the impedance spectrum measurement and dielectric properties of tomato plants in four modal periods of germination stage were carried out. The stages were namely the seedling stage, flowering and fruit setting stage, and fruiting stage respectively. Impedance spectrum fitting was performed with the ZSimpWin software. Then, the biological circuit model of each tissue of tomato plant was obtained. Next, the parameter inversion was used to calculate the value of each element of the biological circuit model. Lastly, the biological circuit model of the tomato plant body in each period was obtained. Through the charging and discharging test of the model of the tomato plant body at each stage, the corresponding parameter value relationship was obtained according to the capacitance characteristics. This would be compared with the component values obtained from the parameter inversion in the model. Results showed that the errors were all less than 4.8%, which verified the rationality of the model. This system acted as a theoretical guidance for the research on the growth and development of tomato and other plants.

摘要
在番茄植株生长发育过程中，不同细胞或组织会对外部环境信息进行储存，并通过离子运输的形式进行表达。为了更好的研究番茄植株的储存模型，用模态理论的思想对番茄个体组织和整体植株生物电路模型进行研究。基于参数反演理论，在 0.1Hz-1MHz 频率范围内，针对发芽期、幼苗期、开花坐果期、结果期四个模态周期的番茄植株进行阻抗谱测量以及介电特性研究，通过 ZSimpWin 软件进行阻抗谱拟合，得出番茄植株各组织生物电路模型，并利用参数反演计算生物电路模型的各元件值，最终得出各时期番茄植株体的生物电路模型。通过对番茄植株体各时期的模型进行充放电试验，根据电容特性得出相应的参数值关系，与模型中参数反演出的元件值对比验证，其误差均小于 4.8%，验证了模型的合理性。本系统为番茄及其他植株生长发育研究提供理论指导。

INTRODUCTION
With the introduction of the modal idea, it was of great significance to introduce this idea to plants. Modality is a processing process that was introduced to plants. Modality could be understood as the change of ion transport in plant cells or tissues under the input of exogenous factors. This resulted in changes in cells, tissues or structures in the process. Tomato is one of the most typical vegetable plants. Under natural conditions, the changes of exogenous factors such as atmospheric electric field and magnetic field would result in an instantaneous potential difference between the top and the root of the tomato during the growth period. This would then drive the soluble ions in the tomato body. Under the influence of an external electrostatic field, this movement would be accelerated in the form of electrostatic induction force. Hence it would form a larger biological current which promoted the movement and absorption of ions and nutrients, thereby, promoting the growth of plants. Ions in tomato acted as electrical signals of tomato plants, which had a remarkably significant effect on tomato growth (*Chen et al., 2010*).

[1] *Ying Wang, M.S. Stud.; Huifei Yang, M.S. Stud.; Ruijie Xie, M.S. Stud.; Zhenyu Liu, Prof. Ph.D.*

As a method of measuring electrical signals in biological tissues, biological circuit models had been utilized in the field of animals and plants. The plant tissue or organ was replaced by a simple biological circuit model. The parameters in the circuit represented the changes in the morphological structure of the plant organ during the growth process. At present, Schwan (*Schwan et al., 2006; Foster et al., 2000*) had established a spherical single-cell dielectric model from the perspective of electric field. With it, he had deduced the calculation method of cell transmembrane potential under the action of a steady electric field. Hodgkin *(Hodgkin et al., 1952)* proposed the equivalent circuit model of the cell membrane by combining the properties of the cell membrane and its ion channels. In the further study on the relationship between cells, resistance and capacitance, Kanai (*Kanai et al., 1983*) obtained a simple cellular RC circuit model by describing the extracellular fluid, cytoplasmic membrane, and cell contents by parallel capacitance and resistance respectively. The circuit model explained the use of dielectric spectroscopy to characterize the dielectric properties of cells principle. According to Yao Chenguo (*Yao et al., 2006*) under the addition of different frequencies of electrical stimulation, the cell circuit model intuitively reflected the influence of cell membrane potential. With the aim of studying the changes between cells or tissues during tomato growth, this paper proposed a plant biological circuit model to store modal information. The modal information stored in plant cells was presented through the biological circuit model. On this basis, combined with the advantages of electrochemical detection, the acquisition of tomato plant health status information could be attained. This would be able to provide help for plant health status diagnosis and promote agricultural development.

PRINCIPLES OF TOMATO PLANT BIOLOGICAL CIRCUIT MODEL

Tomato plant biological circuit model was based on electrochemical impedance spectroscopy (EIS) technique (*Barsoukov et al., 2005*). It uses the electrical impedance imaging of inverse problems in electromagnetic field, the dielectric constant analysis theory of biological tissues (*Li et al., 2020*), and the equivalent circuit to quantitatively evaluate the electrochemical impedance spectrum data, so as to build a tomato plant biological circuit model (*Wang et al., 2019*). Figure 1 showed the impedance chart that reflected the relationship between the real and imaginary parts of impedance. Each parameter value in the impedance circle diagram represented the impedance characteristic of the biological tissue.

The representations of the characteristic parameters R_0, R_∞ and α were as follows:

$$R_0 = x_0 + \sqrt{r^2 - y_0^2} \tag{1}$$

$$R_\infty = x_0 + \sqrt{r^2 - y_0^2} \tag{2}$$

$$\alpha = 1 - \frac{2}{\pi}\arcsin\left(\frac{|y_0|}{r}\right) \tag{3}$$

$$\tau = \frac{\left(\frac{R_0 - Z_i(\omega_i)}{Z_i(\omega_i) - R_\infty}\right)^{\frac{1}{\alpha}}}{j\omega_i} \tag{4}$$

The characteristic parameters can be obtained by the center coordinates (x_0, y_0) and the radius r of the impedance circle. The parameter τ can be obtained by the above calculation, and x_0, y_0 and r can be calculated according to the least square method.

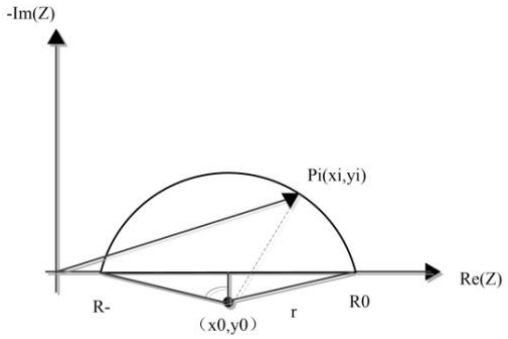

Fig. 1 - Real and imaginary impedance circle diagram

Due to the different external environmental information stored in different biological tissues or structures, the forms of ion transport were different. Hence, the electrical parameters stored in cells were also different. The Cole-Cole theory of bioimpedance established a ternary equivalent circuit model and treated each tissue and organ of a plant as an equivalent circuit (*Wang et al., 2017*) to realize the combination of the ternary equivalent circuit model and the physiology of each plant tissue or organ. Due to the selective permeability of the cell membrane, when a low-frequency AC signal passed through the plant cell, the current would mainly flow from the outside of the cytoplasm. When the frequency gradually increased, the electrical impedance value of the cell membrane would gradually decrease. Electric current passed through the cell membrane to the cell symplast, where it formed a basic parallel circuit of capacitance and resistance (*Lukács et al., 2020*). Therefore, the physiological properties of various tissues or organs of plants could be characterized according to electrical impedance spectroscopy measurements. With the method of parameter inversion, the impedance spectrum curve obtained by the electrical impedance spectrum measurement could be fitted with the basic model. Then, the parameter values in the model can be obtained by the method of parameter inversion.

MATERIALS AND METHODS

Material selection and cultivation

The test samples of plant tomato seeds had utilized tomato plants provided by Shanghai Changzhong Tomato Seed Industry Co., Ltd (Variety: Cooperative 909). They were divided into four different stages. Namely the germination stage, seedling stage, flowering and fruit setting stage, and fruiting stage respectively. In each period, 20 tomato plants in good growth condition were selected for impedance spectroscopy measurement. After the test material was obtained, it would be placed in an incubator. The set temperature of the incubator would be set at 25°C with the humidity at 42%RH and the light at 30000Lx. After the seeds had germinated, they were transferred to room temperature to continue growing.

Impedance spectroscopy

Impedance measurement was performed by adopting the Gamry Framework software installed by the Interface 1000 electrochemical workstation (Gamry, USA) using tomato impedance spectroscopy and parameter setting (*Väinölä et al., 2000; Wang et al., 2019*). By taking 71 frequency points in the frequency range of 0.1Hz - 1MHz (Initial Freq: 1MHz, Final Freq: 0.1Hz), the impedance spectrum data density (Points/Decade) is set to 10 while the AC voltage (AC Voltage, unit: (mV rms)) RMS value is set to 10mV. The default value of electrode active area (Area) is 1. The measured data would be automatically saved to the Gamry Echem Analyst software for analysis through the interface. Then, the impedance spectrum of each tissue would be obtained.

Construction of impedance characteristic model of tomato tissues

Dielectric properties differed between different biological tissues of tomato. Therefore, the model construction of the impedance characteristics of tomato plants would require analysis and examination by sub-organizations, namely tomato plant tissue, roots, stems, branches and leaves all composed of cells. The cell wall was one of the principal substances that made up the cells of each tissue of the plant. Due to the selective permeability of cell membranes, impedance characteristics could be modeled for each cell in plant tissue. In Figure 2(a), R_e represents the resistance of the extracellular fluid, Ce is the capacitance of the extracellular fluid while R_m is the resistance of the cell membrane. Cm refers to the capacitance of the cell membrane, Ri is the resistance of the intracellular fluid, and Ci refers to the parallel capacitance of the extracellular fluid (*Mao et al., 2014*). When the frequency was less than 1MHz, the resistance of the cell membrane would become larger, and the branch where the resistance Rm was located would be regarded as an open circuit. Utilizing the equivalent principle of the circuit, a certain part of the circuit would be simplified, and the volt-ampere characteristics on its port remained unchanged in Figure 2(b). Ri, Re, Cm representing the internal and external fluid resistance and membrane capacitance of biological tissue respectively.

(a) Single Cell Equivalent Circuit Model *(b) Single Cell Equivalent Circuit Simplified Model*

Fig. 2 - A biological circuit model of a single cell in biological tissue

Impedance spectrum fitting

In order to better complete the impedance spectrum fitting process, the model simulation software ZSimpWin was utilized to realize the process (*Rangadhar et al., 2021*). (1) Input the impedance data measured at the roots, stems and leaves of tomato plants into the software to automatically draw the corresponding impedance curves. (2) Select the equivalent circuit model corresponding to each tissue for curve fitting. Next, make corresponding modifications to the model according to the test values. Lastly, compare the test values of each model and determine the equivalent circuit model of each tissue of the plant. (3) According to the determined equivalent circuit model, the corresponding parameter values in the model are obtained through automatic iteration.

Construction of tomato whole plant biological circuit model

Explore the connection between organizations according to the principle of two-port network and equivalent circuit (*Song et al., 2009*). Explore the construction of a biological circuit model of the whole tomato plant and observe how it fitted the biological circuit model. Then, the parameters were inverted to obtain the value of each component. Next, the model would be verified to determine the circuit model of the whole plant. In order to ensure the accuracy of the verification model, impedance spectrum fitting was performed on the four stages of the tomato plant: germination stage, seedling stage, flowering and fruit setting stage, and fruiting stage respectively. Lastly, the ZSimpWin software was utilized to perform model fitting analysis to obtain test values and related parameters. The correctness of the tomato plant biological circuit model would be verified by stages.

RESULTS AND DISCUSSION

Tomato tissue biological circuit model

Impedance spectrum characteristics of tomato tissues

The impedance spectrum curve of each tissue of tomato is shown in Figure 3. From the root Bode plot (Figure 3(b)) it could be observed that the impedance values were higher at frequencies between 100MHz-10kHz (*Rajkai et al., 2005*). When the frequency was between 10kHz-1MHz, the impedance amplitude gradually decreased. By observing Figure 4(d), when the frequency was less than 10kHz, it would belong to the high impedance frequency band. When the frequency was greater than 10kHz but lesser than 1MHz, the impedance amplitude altered from high to low value. From Figure 4(f) can be observed that the impedance of the bottom leaf was the largest followed by the impedance of the parietal leaf in the second place. Lastly, the impedance of the middle leaf would be the smallest. By observing the impedance spectra of roots, stems and leaves, it is discovered that when the current frequency gradually increased, the phase angle gradually reached the highest point first.

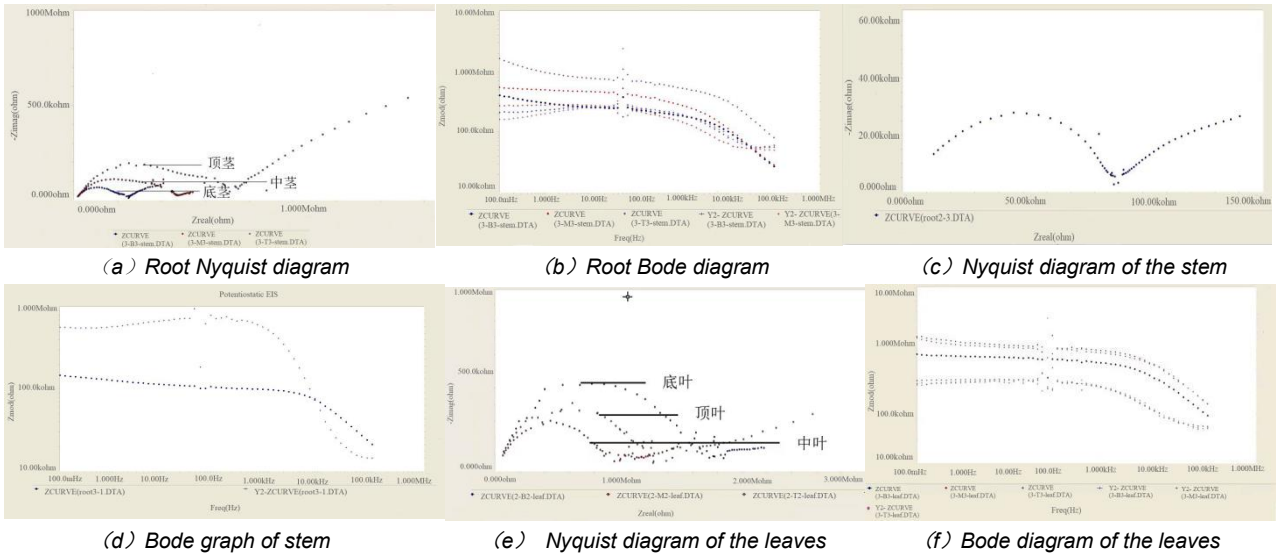

(a) Root Nyquist diagram *(b) Root Bode diagram* *(c) Nyquist diagram of the stem*

(d) Bode graph of stem *(e) Nyquist diagram of the leaves* *(f) Bode diagram of the leaves*

Fig. 3 - Impedance profile of each tissue in tomato

When it was close to the 10kHz frequency point, it would demonstrate an upward trend. According to the analysis curve of the root Nyquist in Figure 4(a) and comparing the four models, the root impedance characteristic model was more in line with the double-DCE model (*Yang et al., 2011; Zhang et al., 2009; Zhang et al., 2005; Wang et al., 2010; Liu et al., 2017*). It could be observed from Figure 4(c) that the impedance

values of the stems of different parts of the tomato plant displayed obvious changes. The result could also be deduced from Figure 4(e). It showed that the impedance values of the leaves of different parts of the tomato plant also had obvious changes. This provided a theoretical basis for the sub-section measurement of tomato stems and leaves (*Xing et al., 2021*).

Construction of biological circuit models of tomato tissues

The ZSimpWin software was utilized to analyze the data measured by the impedance map of each tomato tissue. The R(CR)(CR)) circuit model was fitted with the data measured by the root experiment. The Chisq is 0.0165 when using capacitance C test. Since the time constant of the root impedance spectrum curve was relatively scattered, in the constant phase angle element (CPE) fitting process (*Liu et al., 2012*), R(Q(R(QR))) (Figure 4(a)), the number of iterations of the biological circuit model Iter was 6 with the test value of Chisq at 0.00107. By comparing the test values, it was discovered that the fitting effect of the capacitor C was worse than that of the constant phase angle element CPE. The biological circuit model form of R(Q(R(QR))) was more in line with the actual root impedance characteristics. With the similar root fitting method, the stem R(QR(QR)) biological circuit model in Figure 3(b) possessed the best fitting effect. The leaf R(QR(QR)(CR)) biological circuit model in Figure 3(c) was in line with the actual circuit.

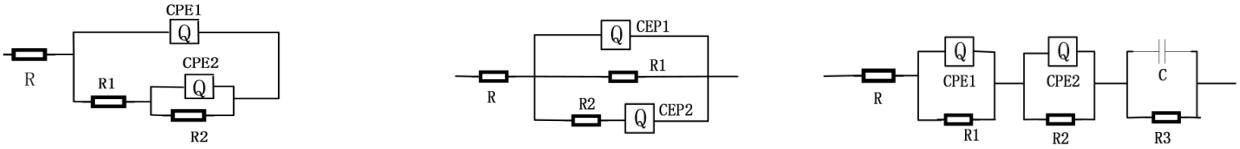

(a) R(Q(R(QR))) biological circuit model *(b) R(QR(QR))biological circuit model* *(c) R(QR(QR)(CR))biological circuit model*

Fig. 4 - Biological circuit model of each tissue in tomato

Establishment of tomato whole plant biological circuit model

Biological circuit model of tomato plants in different periods

In order to further strengthen the accuracy of model validation, impedance spectrum fitting was performed on the four stages of the tomato plant: germination stage, seedling stage, flowering and fruit setting stage, and fruiting stage respectively. The ZSimpWin software was utilized for model fitting analysis, and the test values and related parameters were obtained. At the germination stage of tomato plants, sampling measurements were made to obtain R(Q(R(CR))), R(QR(CR)(CR)), R(QR)(QR)(CR), R(QR)(QR) test values which were 0.0285, 0.00137, 0.00156, 0.00146 respectively. It is proved by referring to relevant data that when the test value is less than 0.01, the fitting effect is good. The smaller the test value, the better the fitting effect. The fitting result is shown in Figure 5. The biological circuit model of the tomato plant at the germination stage was R(QR(CR)(CR)) in Figure 6(a). Similar to the above results, the biological circuit model of the tomato plant body at the seedling stage was R(QR(CR)(CR)). The impedance spectrum model of the plant body at the flowering, fruit setting and fruiting stages was R(Q(R(CR))) in Figure 6(b).

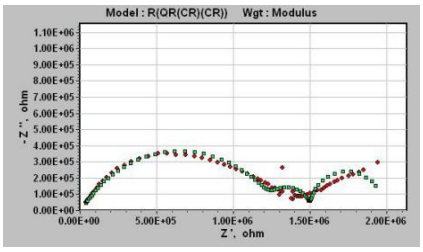

(a) Fitting results of impedance spectrum of tomato plants at germination stage

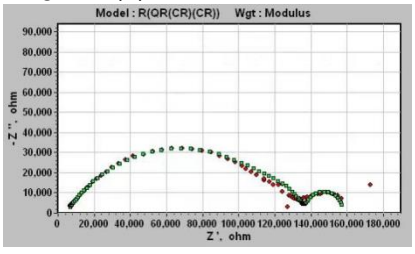

(b) Fitting results of impedance spectrum of tomato plants at seedling stage

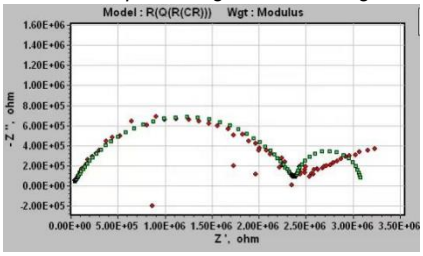

(c) Fitting results of impedance spectrum of tomato plants during flowering and fruit setting

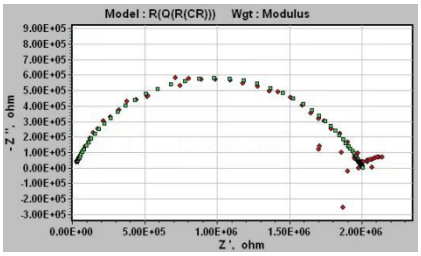

(d) Fitting results of impedance spectrum of tomato plants during the fruiting period

Fig. 5 - Results of fitting of impedance profiles of tomato plants

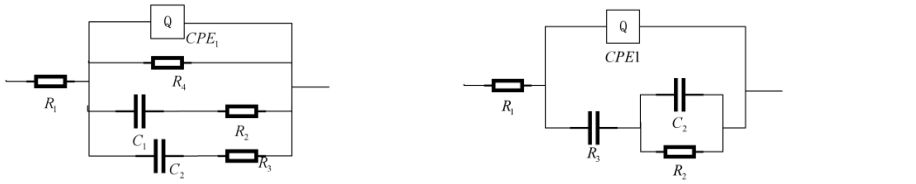

(a) R(QR(CR)(CR)) biological circuit model *(b) R(QR(CR)(CR)) biological circuit model*

Fig. 6 - Biological circuit model of different periods of tomato

Parameter inversion of biological circuit model in different periods of tomato

According to the test value of tomato germination stage ChiSp=0.00137, from the data displayed in Table 1, it could be concluded that the error of each parameter value was less than 0.048. This indicated that the R(QR(CR)(CR)) model was consistent with the impedance characteristics of tomato plants at the germination stage. Similarly, the R(QR(CR)(CR)) model conformed to the impedance characteristics of tomato plants at the seedling stage in Table 2. The R(Q(R(CR))) model was consistent with the impedance characteristics of tomato plants in flowering in Table 3 and fruit-setting and fruiting stages in Table 4.

Table 1

Inversion results of impedance spectrum parameters in germination stage

Parameter	Starting value	Termination value	Error (%)
R(ohm.cm^2)	3089	3089	2.239
Q(S-sec^n/cm^2)	5.72E-10	5.72E-10	4.372
n(0<n<1)	0.660	0.660	1.121
R(ohm.cm^2)	1.97E+03	1.97E+03	1.997
C(F/cm^2)	3.25E-11	3.25E-11	2.110
R(ohm.cm^2)	9.11E+03	9.11E+03	4.754
C(F/cm^2)	6.87E-08	6.88E-08	1.577
R(ohm.cm^2)	3.18E+03	3.18E+03	4.552

Table 2

Inversion results of impedance spectrum parameters in seedling stage

Parameter	Starting value	Termination value	Error (%)
R(ohm.cm^2)	5195	5197	4.718
Q(S-sec^n/cm^2)	2.12E-08	2.12E-08	1.476
n(0<n<1)	0.597	0.597	2.032
R(ohm.cm^2)	1.54E+03	1.54E+03	2.141
C(F/cm^2)	4.99E-11	4.99E-11	4.183
R(ohm.cm^2)	2.32E+03	2.32E+03	3.725
C(F/cm^2)	2.78E-07	2.78E-07	3.725
R(ohm.cm^2)	5.02E+03	5.02E+03	1.529

Table 3

Inversion results of impedance spectrum parameters during flowering and fruit setting

Parameter	Starting value	Termination value	Error (%)
R(ohm.cm^2)	12200	12200	3.952
Q(S-sec^n/cm^2)	5.71E-10	5.71E-10	1.76
n(0<n<1)	0.800	0.800	2.158
R(ohm.cm^2)	2.40E+03	2.40E+03	2.283
C(F/cm^2)	2.90E-07	2.90E-07	3.298
R(ohm.cm^2)	6.80E+03	6.80E+03	1.771

Table 4

Inversion results of impedance spectrum parameters during the result period

Parameter	Starting value	Termination value	Error (%)
R(ohm.cm^2)	10180	10180	3.474
Q(S-sec^n/cm^2)	6.84E-10	6.84E-10	3.327
n(0<n<1)	0.6489	0.6488	4.763
R(ohm.cm^2)	2.76E+03	2.75E+03	3.486
C(F/cm^2)	1.76E-11	1.76E-11	2.423
R(ohm.cm^2)	1.73E+06	1.73E+06	4.135

MODEL VALIDATION

In order to effectively verify the accuracy of the tomato whole plant model, the tomato plants were sampled in four periods. During the verification, the stable voltage of the power supply is 10V, and the frequency is stable at 10Hz. Connect the two ends of the tomato plant to the multimeter. A 10kΩ resistance is connected in series beside the power supply voltage to preliminarily measure the charging and discharging time of tomato plants and determine the charging and discharging time. Then the charge and discharge experiments were completed respectively. Next, an analysis on the charge-discharge situation of the tomato plant within 30 seconds was conducted. Then, the charge-discharge curve was drawn. It was combined with the impedance model at the germination stage and seedling stage of the tomato plant and its charge and discharge conditions. Figure 7(a), 7(b) and Figure 8(a), 8(b) show the average value of charge and discharge at the germination stage and the seedling stage. According to the characteristics of the capacitor, the capacitor was in a short-circuit state at the moment when the capacitor began to charge. Based on the voltage division formula, the voltage across the tomato plant could be calculated separately at the germination stage and the seedling stage. When t=0, V was the voltage across the tomato plant at t=0.

$$V_{(t=0)} = 10V \times \left[\frac{R_1(R_2 \,//\, R_3)}{R_1(R_2 \,//\, R_3) + 10K\Omega} \right] \tag{5}$$

According to formula 5, the resistance value of resistor R_1 in series with two parallel resistors $R_2 \,//\, R_3$ can be found: $R_1(R_2//R_3)$. Since the capacitor is fully charged, the branch where the capacitor is located will form an open circuit. Similarly, according to the voltage division formula, t_1 is the discharge completion time of the capacitor, V' is the voltage across the tomato plant at t = 0, R_1R_4 is the value of the resistors R_1 and R_4 in series, namely:

$$V' = \frac{(10V \times R_1R_2)}{10K\Omega + R_1R_2} \tag{6}$$

According to formula 6, the series resistance value of R_1 and R_4 can be obtained: $R_1 + R_4$, and the value of $R_1(R_2//R_3)$ and $R_1 + R_4$ can be calculated. Then, a comparative analysis was carried out with the values of each element (Table 1, Table 2) inversion of the model parameters to verify the correctness of the equivalent impedance model at the germination stage and seedling stage of the tomato plant. The verification results were displayed in Table 5.

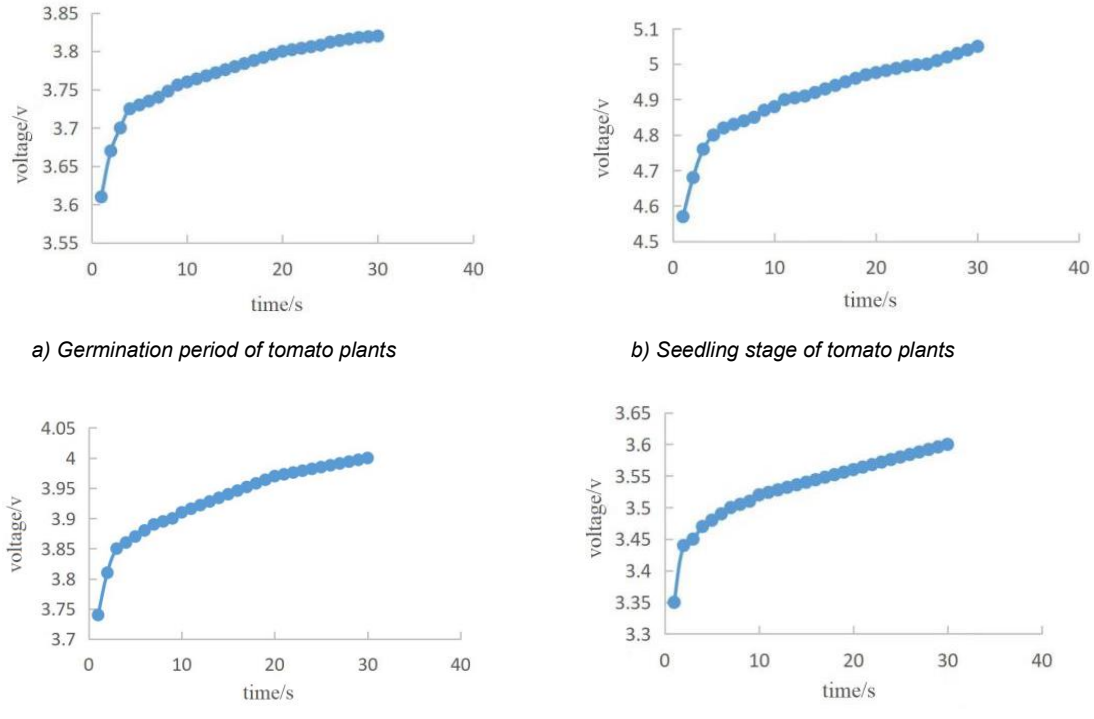

a) Germination period of tomato plants

b) Seedling stage of tomato plants

c) Flowering and fruiting stages of tomato plants

d) Results period of tomato plants

Fig. 7 - Mean charging voltage of tomato plants

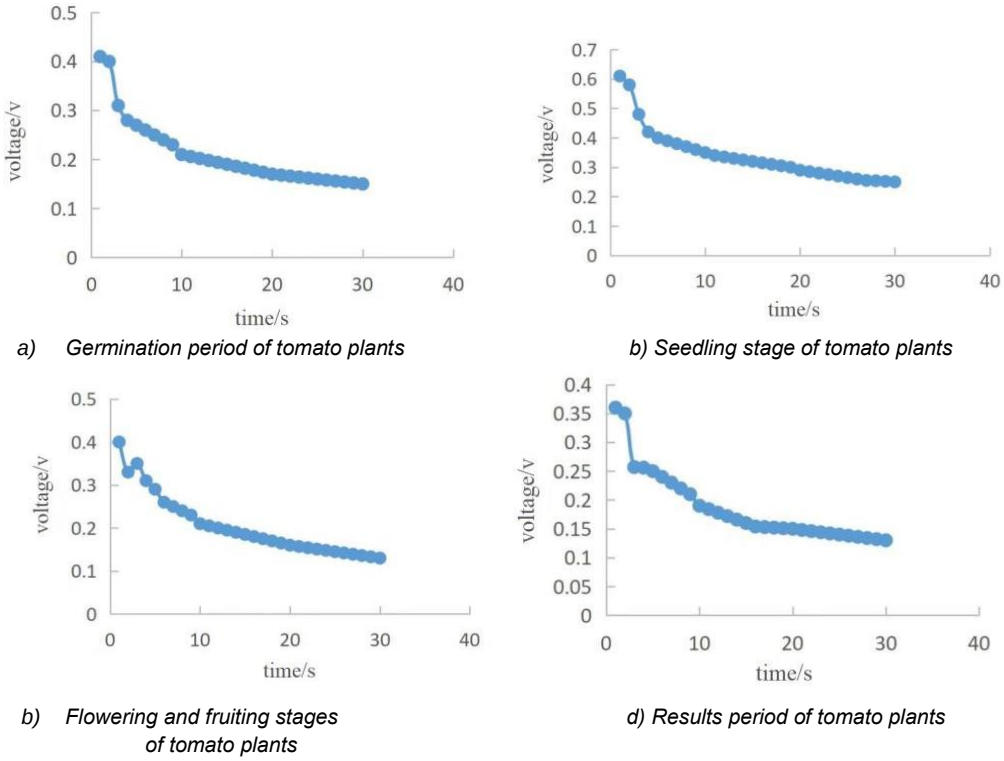

a) Germination period of tomato plants

b) Seedling stage of tomato plants

b) Flowering and fruiting stages of tomato plants

d) Results period of tomato plants

Fig. 8 - Mean discharge voltage of tomato plants

Combine impedance model of tomato plant flowering, fruit setting, fruiting period and its charge and discharge conditions (*Pankaj et al., 2010*). Then compare and analyze with the value of each element inversion of the model parameters in Table 3 and Table 4. to verify the correctness of the biological circuit model at the germination stage and seedling stage of the tomato plant. The verification results were displayed in Table 6.

Table 5

Contrastive analysis of inversion values and measured values of parameters at germination and seedling stages

	Germination stages		Seedling stages	
	$R_1(R_2 // R_3)$	R_1+R_4	$R_1(R_2 // R_3)$	R_1+R_4
Parameter inversion value/Ω	6269	6269	6123	10217
Measurement value/Ω	6075	6129	6330	10725
Error value/%	3.3	2.3	3.2	4.7

Table 6

Comparative analysis of the inversion values and measured values of the parameters at the flowering and fruit setting and fruiting stages

	Fruit setting stages		Fruiting stages	
	R_1+R_2	R_1	R_1+R_2	R_1
Parameter inversion value/Ω	14600	12200	12940	10180
Measurement value/Ω	14100	11900	12430	9860
Error value/%	3.4	2.4	4.0	3.1

By observing the above results, it could be observed that the error between the parameter inversion value and the measured value was less than 4.8%. Within the considered error range, the analysis reviewed that the reason for the error was due to the difference between the capacitive element and the constant phasor element. Then, the accuracy of the tomato plant germination stage, seedling stage, flowering and fruit setting stage, and fruiting stage model could be verified. The conclusions would then be established. The biological circuit model of tomato plant germination stage and seedling stage was R(QR(CR)(CR)), while the biological circuit model of flowering and fruit-setting stage and fruiting stage was R(Q(R(CR))).

CONCLUSIONS

(1) In order to explore the growth and development of tomato plants, this paper proposed to utilize storage modal information as a new method to examine the tomato plants. Due to the differences between different biological tissues or structures, the best choice was to simulate the tissues and organs of each organism with the biological circuit model in physics. The modal information stored in each cell in the plant had its own electrical properties and could be replaced by the equivalent circuit of parallel capacitance and resistance in physics. Therefore, it could transform abstract concepts into concrete models.

(2) By studying the impedance characteristics of tomato plants in different periods, an impedance model was constructed. The ZSimpWin software was adopted to conduct impedance spectrum analysis to discover the optimal biological circuit model. Combined with the theoretical analysis of the two-port network, the connection mode of the biological circuit model of each tissue of the tomato plant was analyzed. The impedance spectrum fitting of the model was then carried out to obtain the results at the germination stage, seedling stage, flowering and fruit setting stage and fruiting stage of the tomato plant. The biological circuit model of the period was obtained, and the component values of each model in each period of the tomato plant were inverted.

(3) During the charging and discharging experiments of tomato plants in different periods, the models of tomato plants in different periods were verified. The results showed that the errors were all less than 4.8%. Through the thorough analysis of the error results, it was discovered that the error was caused by the capacitance element and the differences of constant phasor elements. Hence, the biological circuit model was proved to be reasonable.

REFERENCES

[1] Cao, Y., Repo, T., Silvennoinen, R., Lehto, T., & Pelkonen, P. (2011). Analysis of the willow root system by electrical impedance spectroscopy. *Journal of experimental botany*, 62(1), 351-358.

[2] Chen, S., Li, X., Liu, Y., Tai, P., & Liu, B. (2010). Effect of spatial electric field on soil moisture and barley growth (空间电场对土壤水分和大麦生长的影响). *Transactions of the Chinese Society of Agricultural Engineering*, 26(2), 59-63.

[3] Foster, K. R. (2000). Thermal and nonthermal mechanisms of interaction of radio-frequency energy with biological systems. *IEEE Transactions on Plasma Science*, 28(1), 15-23.

[4] Grosse, C., & Schwan, H. P. (1992). Cellular membrane potentials induced by alternating fields. *Biophysical journal*, 63(6), 1632-1642.

[5] Hodgkin, A. L., & Huxley, A. F. (1952). A quantitative description of membrane current and its application to conduction and excitation in nerve. *The Journal of physiology*, 117(4), 500.

[6] Kanai, H., Sakamoto, K., & Haeno, M. (1983). Electrical measurement of fluid distribution in human legs: estimation of extra-and intra-cellular fluid volume. *Journal of microwave power*, 18(3), 233-243.

[7] Lukács, Z., & Kristóf, T. (2020). A generalized model of the equivalent circuits in the electrochemical impedance spectroscopy. *Electrochimica Acta*, 363, 137199.

[8] Liu Kaiyue, Meng Yu, Lin Shengwei, Cao Yu, Liu Dongyun. (2017). Effects of Drought Stress on Parameters of Electrical Impedance Spectra and Membrane Permeability of Nepeta Leaves (干旱胁迫对荆芥叶片电阻抗图谱参数及膜透性的影响). *Journal of Hebei Agricultural University*, 40(5), 55-59.

[9] Liu Weiqing, Zhou Ming, Liang Zhongguan. (2012). Characteristic simulation and application of constant-phase elements in dye-sensitized solar cells (染料敏化太阳电池中常相角元件特性模拟及应用研究). *Journal of Nanchang Hangkong University (Natural Science Edition)*, 26(03):57-62.

[10] Li Yang, Wang Yongqian, Zhao Pengfei, Wang Nan, Huang Lan, Wang Zhongyi. (2020). Design and experiment of electrical impedance imaging system in plant root zone (植物根区电阻抗成像系统设计与实验). *Journal of Agricultural Machinery*, 51(S1):348-356.

[11] Macdonald, J. R., & Barsoukov, E. (Eds.). (2018). *Impedance spectroscopy: theory, experiment, and applications*. John Wiley & Sons.

[12] Mao Guangjin, Shen Linyong, Zhang Yuhui, Jin Dingyi. (2014). Design and research of bioelectrical impedance measurement experiment. *Industrial Control Computer*, (1), 57-58.

[13] Pradhan, R., Raisa, S. A., Kumar, P., Kalkal, A., Kumar, N., Packirisamy, G., & Manhas, S. (2021). Optimization, fabrication, and characterization of four electrode-based sensors for blood impedance measurement. *Biomedical Microdevices*, 23(1), 1-9.

[14] Pankaj, S. K., Misra, N. N., & Cullen, P. J. (2013). Kinetics of tomato peroxidase inactivation by atmospheric pressure cold plasma based on dielectric barrier discharge. *Innovative Food Science & Emerging Technologies*, 19, 153-157.
[15] Rajkai, K., Végh, K. R., & Nacsa, T. (2005). Electrical capacitance of roots in relation to plant electrodes, measuring frequency and root media. *Acta Agronomica Hungarica*, 53(2), 197-210.
[16] Song Jinyan. (2009). Calculation of two-port network parameters (二端口网络参数的计算). *Science and Technology Information*, (32): 510-511.
[17] Väinölä, A., & Repo, T. (2000). Impedance spectroscopy in frost hardiness evaluation of Rhododendron leaves. *Annals of Botany*, 86(4), 799-805.
[18] Wang Aifang. (2010). Comparative Study on Electrical Impedance and Physiological Indexes of White Bark Pine Seedlings under Drought Stress (干旱胁迫下白皮松苗木电阻抗及生理指标的比较研究). *Hebei Agricultural University*.
[19] Wang Ke, Chen Xuejiao, Xu Xiaowei, Liu Guangqi, Zou Dexu. (2017). Influence of temperature on parameters of Cole-Cole dielectric model of oil-immersed casing (温度对油浸式套管 Cole-Cole 介电模型参数的影响). *Southern Power Grid Technology*, 11(06):42-48.
[20] Wang Yongqian, Zhao Pengfei, Fan Lifeng, Wang Ziyang, Huang Lan, Wang Zhongyi. (2019). Study on compensation and coupling methods in impedance spectroscopy measurement of matrix root zone (基质根区阻抗谱测量中补偿和耦合方法研究). *Journal of Agricultural Machinery*, 50(06):288-298.
[21] Wang, Y. Q., Zhao, P. F., Fan, L. F., Zhou, Q., Wang, Z. Y., Song, C., ... & Wang, Z. Y. (2019). Determination of water content and characteristic analysis in substrate root zone by electrical impedance spectroscopy. *Computers and Electronics in Agriculture*, 156, 243-253.
[22] Xing, D., Chen, L., Wu, Y., & Zwiazek, J. J. (2021). Leaf physiological impedance and elasticity modulus in Orychophragmus violaceus seedlings subjected to repeated osmotic stress. *Scientia Horticulturae*, 276, 109763.
[23] Yao Chenguo, Li Chengxiang, Sun Caixin, MiYan, Mo Dengbin. (2006). Pulse electric field-induced electroporation model of inner and outer membranes and simulation of transmembrane potential. *Chinese Journal of Electrical Engineering,* 26(13): 123-128.
[24] Zhang Gang, Xiao Jianzhong, Chen Duanfen. (2005). Electrical Impedance Spectroscopy Method for Determination of Plant Cold Resistance (测定植物抗寒性的电阻抗图谱法). *Chinese Journal of Plant Physiology and Molecular Biology*, (01): 19-26.
[25] Zhang Jun, Zhao Huijuan, Zhang Gang, Yang Minsheng. (2009). Application of electrical impedance mapping method in determination of cold resistance of Robinia pseudoacacia germplasm resources (电阻抗图谱法在刺槐种质资源抗寒性测定中的应用). *Journal of Plant Genetic Resources*, 10(03): 419-425.